Proceedings of the 18th World Congress
The International Federation of Automatic Control
Milano (Italy) August 28 - September 2, 2011

A UNIFIED MODEL FOR ELECTRICITY AND HYDROGEN PRODUCTION IN MICROBIAL ELECTROCHEMICAL CELLS

R. P. Pinto[a,b], B. Srinivasan[b], and B. Tartakovsky[a,b*]

[a]Biotechnology Research Institute, National Research Council, 6100 Royalmount Ave., Montréal, Que., Canada H4P 2R2 (Boris.Tartakovsky@cnrc-nrc.gc.ca Tel: 1-514-496-2664)
[b]Departement de Génie Chimique, École Polytechnique Montréal, C.P.6079 Succ., Centre-Ville Montréal, Que., Canada H3C 3A7 (e-mails: roberto.pinto@polymtl.ca; bala.srinivasan@polymtl.ca)

Abstract: This work presents a unified dynamic model describing Microbial Fuel Cells and Microbial Electrolysis Cells (MxCs). The same set of kinetic equations is used to describe microbial activity in the anodic compartment of a microbial fuel cell and a microbial electrolysis cell, while cathodic reactions leading to electricity and hydrogen production are described by their respective dependencies. We present the results of parameter estimation and model validation, and an example of MxC model application for process control purposes.

Keywords: Microbial fuel cell; Microbial Electrolysis Cell; Dynamic model.

1. INTRODUCTION

Electrochemical systems represent a novel alternative for energy recovery from organic waste and biomass residue, where microorganisms can be employed to catalyze electrochemical oxidation-reduction reactions. Microbial electrochemical cells such as Microbial Fuel Cells (MFCs) and Microbial Electrolysis Cells (MECs) are among such bio-electrochemical systems. Together, MFCs and MECs could be represented by the acronym MxC. Performance of MxCs largely depends on anaerobic biofilm occupied by anodophilic (electrogenic) microorganisms, which transfer electrons to the anode during their metabolism (Bond et al. 2002). Though anodic compartments in all MxCs are similar, the cathode reactions differ. MFCs operate with cathodes exposed to air resulting in oxygen reduction reaction at the cathode and electricity production (Logan et al. 2006). In contrast, MECs require a small additional input of electrical energy provided by an external power supply to facilitate the reaction of hydrogen formation on the cathode (Rozendal et al. 2006).

Successful development and operation of MxCs requires knowledge of the processes of electron transfer by the microorganisms (Reguera et al. 2005), operating conditions (Aelterman et al. 2008), and suitable external resistance (Woodward et al. 2010). One solution for the complex problems posed by MxCs is to build a mathematical model that can be used to optimize MxC design and operating conditions, as well as to maximize anodophilic microbial activity, and to develop process control strategies.

Despite their importance, few MFC models are presented in the literature, while no MEC models are available. The processes of electron transfer (Marcus et al. 2007) and power generation (Zeng et al. 2010) have been modeled before, but did not take into account the microbial competition for a common source of carbon. Recently, we presented a MFC model that can describe the competition between anodophilic and methanogenic microorganisms (Pinto et al. 2010b). This model has been used to study the influence of external resistance (R_{ext}) on biofilm growth in a MFC, showing the key role of this variable (Pinto et al. 2010a; Pinto et al. 2010c).

In the study presented below, we continue the subject of MxC modeling by presenting a unified model capable of describing electricity and hydrogen production. Results of model validation for both MFC and MEC modes of operation are presented and the perspectives of MxC model application for process design, optimization, and control are discussed.

2. MODEL FORMULATION

The model equations presented here are based on the two-population MFC model developed by Pinto et al. (2010b), which described the competition between anodophilic and methanogenic bacteria for acetate. This model is now expanded with an objective to simulate both electricity and hydrogen production with a relatively simple, fast convergence dynamic model.

The MxC model considers the existence of anodophilic and methanogenic (acetoclastic and hydrogenotrophic) populations and takes into account acetate as the only carbon source supplied to the MxC. Modeling of biofilm formation is simplified by dividing the biofilm into two distinct layers and assuming a homogeneous distribution of microorganisms within each layer (Rauch et al. 1999). The biofilm growing on the anode surface (first biofilm layer) is assumed to consist of anodophilic and acetoclastic methanogenic microorganisms. The former are capable of utilizing the anode as a terminal electron acceptor while the latter produce methane. The charge transfer mechanism from a carbon source to the anode is assumed to involve an intracellular mediator, which exists in the reduced and oxidized forms (Pinto et al. 2010b). It is assumed that the second biofilm layer is located at the cathode surface. This biofilm consists of hydrogenotrophic methanogens, which convert hydrogen produced at the

cathode into methane. The proposed conceptual model is summarized in Fig. 1.

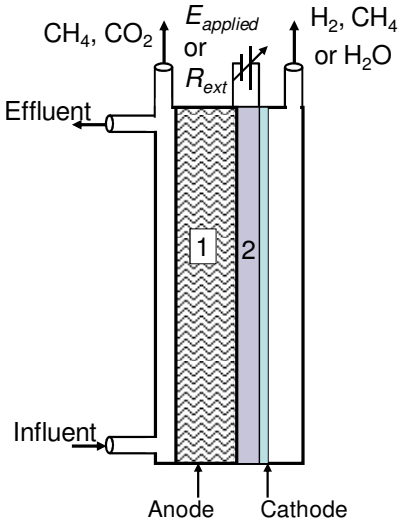

Figure 1. A simplified diagram of the MxC model. Layer 1 represents the anode biofilm, occupied by anodophilic and acetoclastic methanogenic microorganisms, while layer 2 represents the cathode biofilm populated by hydrogenotrophic methanogenic microorganisms.

The following assumptions were made:
1. acetate is assumed to be the only carbon source;
2. the carbon source is well distributed in the anodic compartment, therefore ideal mixing is assumed and acetate gradient in the biofilm is neglected;
3. uniform distribution of microbial populations in the biofilm is assumed and biomass retention due to biofilm formation is described by a hybrid model with growth-washout phases as described below;
4. a constant pool of intracellular electron transfer mediator in anodophilic microorganisms is assumed;
5. biomass growth in the anodic liquid is assumed to be negligible due to short hydraulic retention times used for MxC operation (washout conditions);
6. instant gas transfer from liquid to gas phases is assumed;
7. temperature and pH are considered fully controlled and kept constant.

The acetate and intracellular mediator transformations by three microbial populations can be described by the following transformations:
Anodophilic microorganisms:

$$C_2H_4O_2 + 2H_2O + 4M_{ox} \rightarrow 4M_{red} + 2CO_2 \quad (1)$$

$$4M_{red} \rightarrow 4M_{ox} + 8e^- + 8H^+ \quad (2)$$

where A represents acetate; and M_{red} and M_{ox} are the reduced and oxidized forms of the anodophilic intracellular mediator, respectively.
Acetoclastic methanogenic microorganisms:

$$C_2H_4O_2 \rightarrow CH_4 + CO_2 \quad (3)$$

Hydrogenotrophic methanogenic microorganisms:

$$CO_2 + 4H_2 \rightarrow CH_4 + 2H_2O \quad (4)$$

For a continuous flow MxC considering that the influent and effluent flow rates are the same, the following acetate and microorganisms' material balances can be written:

$$\frac{dA}{dt} = -q_a x_a - q_m x_m + D(A_0 - A) \quad (5)$$

$$\frac{dx_a}{dt} = \mu_a x_a - K_{d,a} x_a - \alpha_1 x_a \quad (6)$$

$$\frac{dx_m}{dt} = \mu_m x_m - K_{d,m} x_m - \alpha_1 x_m \quad (7)$$

$$\frac{dx_h}{dt} = \mu_h x_h - K_{d,h} x_h - \alpha_2 x_h \quad (8)$$

where A and A_0 are the acetate concentration in the anodic compartment and in the influent, respectively [mg-A L^{-1}]; x_a, x_m, and x_h are the concentration of anodophilic, acetoclastic, and hydrogenotrophic microorganisms, respectively [mg-x L^{-1}]; t is the time [d]; q_a, and q_m are the acetate consumption rates by the anodophilic and acetoclastic microorganisms, respectively [mg-A mg-x^{-1} d^{-1}]; μ_a, μ_h, and μ_m are the growth rates [d^{-1}]; D is the dilution rate [$D=F_{in}$ V^{-1}], F_{in} is the incoming flow [L d^{-1}], V is the anodic compartment volume [L]; K_d is the decay rate [d^{-1}]; and α_1, α_2 are the dimensionless biofilm retention constants for layers 1 and 2, respectively.

Biofilm formation and retention in each biofilm layer is based on a two-phase biofilm growth model (Pinto et al. 2010b). Each layer is assumed to hold not more than a maximum attainable biomass concentration (X_{max}) and as the biofilm approaches its steady state thickness a stationary phase is assumed (Wanner and Gujer 1986). The biofilm retention constants can be defined as:

$$\begin{cases} \alpha_1 = \dfrac{(\mu_a - K_{d,a})x_a + (\mu_m - K_{d,m})x_m}{(x_a + x_m)} & if \quad x_a + x_m \geq X_{\max,1} \\ \alpha_1 = 0 \quad otherwise \\ \alpha_2 = \mu_h - K_{d,h} \quad if \quad x_h \geq X_{\max,2} \\ \alpha_2 = 0 \quad otherwise \end{cases} \quad (9)$$

where X_{max} is the maximum attainable biomass concentration of the biofilm layer (1 or 2) [mg-x L^{-1}].

The methane production rates in biofilm layers 1 and 2 can be described by the following balance equations:

$$Q_{CH4\_1} = Y_{CH4} q_m x_m V \quad (10)$$

$$Q_{CH4\_2} = Y_{H2/CH4} Y_h \mu_h x_h V \quad (11)$$

For MEC, the hydrogen production rate is described by:

$$Q_{H2} = Y_{H2}\left(\frac{I_{MEC}}{mF}\frac{RT}{P}\right) - Y_h \mu_h x_h V \quad (12)$$

where Y_{CH4} is the methane yield [mL-CH_4 mg-A^{-1}]; Y_{H2} is the dimensionless cathode efficiency; $Y_{H2/CH4}$ is the yield of methane from hydrogen [mL-CH_4 mg-H_2^{-1}]; I_{MEC} is the MEC current [A]; Y_h is the yield rate for hydrogen consuming methanogenic microorganisms [L mg-x^{-1} d^{-1}]; F is the Faraday constant [A d $mole^{-1}$]; R is the ideal gas constant [L atm K^{-1}

mol^{-1}]; P is the MEC pressure [atm]; and T is the MEC temperature [K].

Intracellular Material Balances of Anodophilic Microorganisms

The following balance equations can be written for each anodophilic microorganism:

$$M_{Total} = M_{red} + M_{ox} \tag{13}$$

$$\frac{dM_{ox}}{dt} = -Y_M \; q_a + \frac{\gamma}{V \; x_a} \frac{I_{MXC}}{m \; F} \tag{14}$$

where M_{ox} is the oxidized mediator fraction per anodophilic microorganism [mg-M mg-x^{-1}]; M_{red} is the reduced mediator fraction per each anodophilic microorganism [mg-M mg-x^{-1}]; M_{Total} is the total mediator fraction per microorganism [mg-M mg-x^{-1}]; I_{MxC} is the MxC current [A]; Y_M is the mediator yield [mg-M mg-A^{-1}]; $\gamma$is the mediator molar mass [mg-M mol$_{med}^{-1}$]; and m is the number of electrons transferred per mol of mediator [mol-e^- mol$_{med}^{-1}$].

Kinetic Equations

By using multiplicative Monod kinetics the following equations can be written:

$$\mu_a = \mu_{\max,a} \frac{A}{K_{A,a} + A} \frac{M_{ox}}{K_M + M_{ox}} \tag{15}$$

$$\mu_m = \mu_{\max,m} \frac{A}{K_{A,m} + A} \tag{16}$$

$$q_a = q_{\max,a} \frac{A}{K_{A,a} + A} \frac{M_{ox}}{K_M + M_{ox}} \tag{17}$$

$$q_m = q_{\max,m} \frac{A}{K_{A,m} + A} \tag{18}$$

where μ_{max} is the maximum growth rate [d^{-1}]; q_{max} is the maximum acetate consumption rate [mg-A mg-x^{-1} d^{-1}]; and K is the half-saturation (Monod) constant [mg-A L^{-1} mg-M L^{-1}].

Hydrogenotrophic methanogens

The hydrogenotrophic methanogens consume hydrogen produced at the cathode. Their growth in biofilm layer 2 (Fig. 1) was assumed to be limited by the saturation concentration of hydrogen in water (1 mg L^{-1}). Furthermore, gas to liquid transfer limitation was neglected so that dissolved hydrogen concentration was assumed to be at its saturation value if hydrogen was produced at the cathode (MEC). When no hydrogen was produced (i.e. MFC), the concentration of dissolved hydrogen is assumed to be equal to zero and therefore the growth rate is equal to zero. This dependence can be represented by:

$$\mu_h = \mu_{\max,h} \frac{H_2}{K_h + H_2}, where \begin{cases} H_2 = H_2^* & if \quad Q_{H2} > 0 \\ H_2 = 0 & if \quad Q_{H2} = 0 \end{cases} \tag{19}$$

where H_2^* is the hydrogen saturation concentration in water [mg-H_2 L^{-1}]; and K_h is the half-saturation (Monod) constant [mg-H_2 L^{-1}]

Electrochemical Equations

MxC voltage can be calculated using theoretical values of electrode potentials and subtracting ohmic, activation, and concentration losses. Therefore the following electrochemical balance can be written (Fuel Cell Handbook 2005):

$$E = E_X - \eta_{ohm} - \eta_{conc} - \eta_{act} \tag{20}$$

where E is the MxC voltage [V]; E_X represents the theoretical electromotive force (E_{EMF}) for the MFC and the counter-electromotive force (E_{CEF}) for the MEC [V]; η_{ohm} is the ohmic over-potential [V]; η_{conc} is the concentration over-potential [V]; η_{act} is the activation over-potential [V].

Ohm's law can be applied in Eq. 20 to compute ohmic losses ($\eta_{ohm} = I_{MxC} R_{\text{int}}$). Concentration losses can be divided between anode and cathode reactant mass transfer processes. Here, concentration losses at the cathode will be neglected due to the small size of protons resulting in a large diffusion coefficient. The concentration losses at the anode can be calculated using the Nernst equation (Pinto et al. 2010b):

$$\eta_{conc,A} = \frac{RT}{mF} \ln\left(\frac{M_{Total}}{M_{red}}\right) \tag{21}$$

where R is the ideal gas constant [J K^{-1}.mol^{-1}], and; T is the MxC anode temperature [K].

Furthermore, activation losses can also be separated between the electrodes. As has been shown before (Pinto et al. 2010b), these losses can be neglected at the anode ($\eta_{act,A} \approx 0$). For the MFC model, cathodic activation losses are considered constant and are included in the computation of open circuit potential (i.e. $E_{OCP} = E_{EMF} - \eta_{act,C}$). The cathodic activation losses for the MEC model can be calculated by the Butler-Volmer equation. Since MECs operate at high over-potential at the cathode (Logan et al. 2008), Butler-Volmer equation can be approximated by (Noren and Hoffman 2005):

$$\eta_{act,C} = \frac{RT}{\beta mF} \sinh^{-1}\left(\frac{I_{MEC}}{A_{sur,A} I_0}\right) \tag{22}$$

where I_0 is the exchange current density in reference conditions [A]; $A_{sur,A}$ is the anode surface area [m^2]; and β is the dimensionless transfer coefficient that represents the activation barrier symmetry. Finally, in Eq.20, Ohm's low can be used to compute the MFC current ($E = I_{MFC} R_{ext}$) and for an MEC, the applied voltage should be negative ($E = - E_{applied}$).

As shown in Pinto et al. (2010b), the concentration losses can be more accurately represented by the addition of boundary conditions at high current densities. To avoid discontinuity when integrating model equations, the boundary conditions were replaced with a Monod-like term that limits calculated MxC current at low values of M_{red}. Therefore, the MFC and MEC current can be calculated by combining Eqs. (20-22):

$$I_{MFC} = \frac{E_{OCP} - \frac{RT}{mF}\ln\left(\frac{M_{Total}}{M_{red}}\right)}{(R_{ext} + R_{\text{int}})} \frac{M_{red}}{\varepsilon + M_{red}} \quad (23)$$

$$I_{MEC} = \frac{E_{CEF} + E_{applied} - \frac{RT}{mF}\ln\left(\frac{M_{Total}}{M_{red}}\right) - \eta_{act,C}(I_{MEC})}{R_{\text{int}}} \frac{M_{red}}{\varepsilon + M_{red}} \quad (24)$$

where ε is a constant [mg-M mg-x^{-1}]; $\varepsilon \sim 0$.

Eq. (23) can be solved analytically, while Eq. (24) can only be solved numerically, the activation losses are depend on the current, $\eta_{act,C}=f(I_{MEC})$, as shown in Eq. (22). To improve model accuracy during the start-up period the E_{OCP} and R_{int} values were linked to the concentration of anodophilic microorganisms as proposed by Pinto et al. (2010b):

$$R_{\text{int}} = R_{MIN} + (R_{MAX} - R_{MIN})e^{-K_R X_a} \quad (25)$$

where R_{MIN} is the lowest observed internal resistance [Ω]; R_{MAX} is the highest observed internal resistance [Ω]; and K_R is the constant, which determines the curve steepness [L mg-x^{-1}];

$$E_{OCP} = E_{MIN} + (E_{MAX} - E_{MIN})e^{\frac{-1}{K_R X_a}} \quad (26)$$

where E_{MIN} is the lowest observed E_{OCP} value [V]; and E_{MAX} is the highest observed E_{OCP} value [V]. The R_{min}, R_{max}, E_{min}, and E_{max} values were obtained from the polarization tests. Parameter K_R was identified using voltage measurements at the beginning of the MFC operation.

Numerical Methods and Calculations

Integration of model equations was performed in MATLAB (Mathworks Inc., Natick, MA, USA). Model parameters were estimated by minimizing the following objective function:

$$F_{obj} = \sum_{i=1}^{m} \frac{w_i}{n_i} \left(\sum_{j=1}^{n_i} \left(\bar{y}_{j,i}^{\exp} - \bar{y}_{j,i}^{sim} \right)^2 \right) \quad (27)$$

where $\bar{y}_{j,i}^{\exp}$ and $\bar{y}_{j,i}^{sim}$ are the normalized experimental and simulated values of the i-th state variable at the j-th sampling time, respectively; w_i is the weight constant of the i-th state variable; n_i is the number of measurements (samples) of the i-th state variable, and m is the number of measurable state variables.

Model outputs were compared with experimental results using the calculations of the adjusted coefficient of determination (R^2) defined as:

$$R^2 = 1 - \frac{1}{n_i} \sum_{j=1}^{n_i} \left(\frac{\bar{y}_i^{\exp} - \bar{y}_i^{sim}}{\max(\bar{y}_i^{\exp}, \bar{y}_i^{sim})} \right)^2 \quad (28)$$

3. PARAMETER ESTIMATION AND VALIDATION

3.1 Microbial Fuel Cell

The model responses will be compared with experimental results obtained in a MFC fed with acetate at three influent concentration levels of 500, 1000, and 2000 mg-A L^{-1}. The anodic compartment was kept at 25°C with a temperature controller. Weekly polarization tests (*PT*) were performed during the experiment, when the R_{ext} was manually decreased from open circuit voltage to low R_{ext} values, with measurements acquired after a delay of 10 min after each resistance change. *PT* test gave information about the open circuit voltage and MFC internal resistance. When *PT* tests were not being performed, the value of R_{ext} was determined by the perturbation observation method (Woodward et al. 2010), which was used to maximize power output. The MFC model ability to predict voltage measurements during on-line control of R_{ext} is therefore evaluated. Detailed experimental design, operation, characterization, and analytical methods can be found in Pinto et al. (2010b).

The same model parameters as in Pinto et al. (2010b) were used for model validation (table 2), except E_{MAX}, which was chosen based on the measured open circuit voltage. Figure 2 shows a comparison of model predictions with the experimental results for acetate effluent and voltage. The peaks in the voltage measurements represent *PT* tests. As one can see, a good agreement was obtained between measured and predicted effluent acetate and output voltage (Fig 2 *a*, and *b*). Even with the R_{ext} variations, output voltage was successfully predicted.

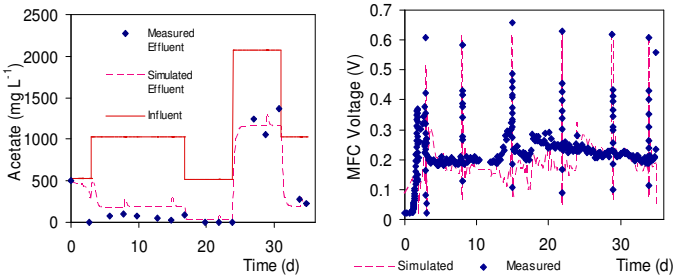

Figure 2. Comparison of model outputs with experimentally measured values in the MFC experiment.

3.2 Microbial Electrolysis Cell

To simulate MEC outputs, parameters of the MxC model described above had to be estimated. Two MEC data sets were required: one for parameters estimation (MEC-1) and the other for model validation (MEC-2). MEC-1 was fed with acetate at three concentration levels: 1000, 1500, and 1900 mg-A L^{-1}, while MEC-2 was fed with acetate at either 1500 or 1900 mg-A L^{-1}. In both tests MECs were kept at 30°C with a temperature controller. The applied voltage was always set to 1 V, except during voltage scan tests. These tests were performed periodically by varying the applied voltage from 1.2 V to 0.3 V with current measurements at each applied voltage. Detailed experimental design, operation,

characterization, analytical measurements, and MEC construction can be found in Manuel et al. (2010).

Because the tests were carried out in MECs that were in operation for over one month prior to the test startup, initial conditions for biomass density were set close to the maximum attainable biomass density (i.e. $x_h \approx X_{max,h}$) and no growth rates could be estimated. Furthermore, no quantifiable methane production in the anode was measured during all tests, apparently because the acetoclastic methanogens were out-competed by the anodophilic microorganisms during MEC operation preceding the test (Pinto et al. 2010c). Therefore, the initial concentration of the acetoclastic methanogenic microorganisms was set to zero ($x_m = 0$). Due to the difference in anodic compartment temperature between MFC and MEC tests (25°C vs 30°C), maximum reaction rates had to be re-estimated. The parameters identified for the MEC model were $q_{max,a}$, Y_M, E_{CEF}, and (Y_h*$X_{max,h}$). Other model parameters were chosen based on Pinto et al. (2010b), table 2.

After selecting the model parameters to be identified, the objective function defined in Eq. (27) was minimized using the Nelder-Mead simplex algorithm implemented in the FMINS subroutine of the MATLAB Optimization Toolbox. The state variables used for the minimization were measured values of acetate concentration, current, hydrogen production, and methane production in the anode and cathode compartments. R^2 values of model outputs for all data sets are provided in Table 1.

Table 1. A comparison of R^2 values calculated for the MFC and MEC data sets used for parameters estimation and model validation.

state variable	*MFC*	*MEC-1*	*MEC-2*
Acetate	0.64	0.68	0.87
Current	0.87	0.75	0.90
H_2 flow	-	0.74	0.99
CH_4 Cathode	-	0.60	0.80
CH_4 Anode	0.79	-	-

Figure 3 presents a comparison of model predictions with the experimental results for acetate and current. The high initial concentration of microorganisms and the constant applied voltage led to constant predicted current, while the measured current was slightly fluctuating due to such factors as variations in cathode chamber pressure and the MEC's internal resistance. Nevertheless, an adequate agreement was obtained between measured and predicted effluent acetate values and current (Table 1).

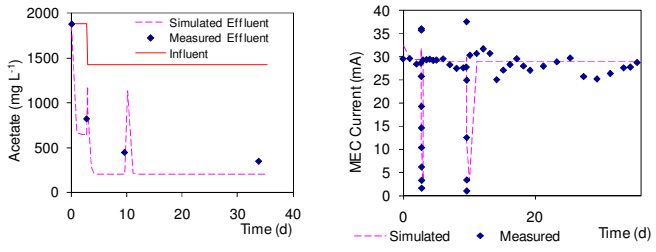

Figure 3. Comparison of model outputs with experimentally measured values for MEC experiment.

4. DISCUSSION

In recent years, there was a significant increase in publications dedicated to MxC microbiology and electrochemistry. However, most of this research was limited to experimental methods thus limiting the ability to apply the acquired knowledge to process control and design, where the existence of an adequate and relatively simple process models is desirable. The MxC model presented above attempts to close this gap by providing a simulation tool that can be used for design, optimization, and control purposes. For example, our MxC model can be used to simulate an integrated process of wastewater treatment and energy production. The optimum treatment capacity (flow rate for a given effluent concentration) could be determined as a function of desired effluent and influent concentrations. However, such optimum flow calculation is bound to present errors in reality, since the model presents many assumptions and parameters such as maximum growth and acetate consumption rates, which are estimated with a certain confidence interval. Another approach would be to control the effluent composition by manipulating the influent flow so that the optimum treatment capacity can be found. A PI controller can be used to maintain a pre-set effluent composition by controlling the influent flow without presenting errors due to parameter estimation uncertainties.

In the example provided below, performance of a MEC and a MFC equipped with a PI controller is simulated during a step decrease in the influent concentration from 1100 to 1000 mg-*A* L^{-1}. In these simulations model parameters were kept as in Table 2. Same controller parameters were used in both simulations. The simulation results are presented in Figure 4.

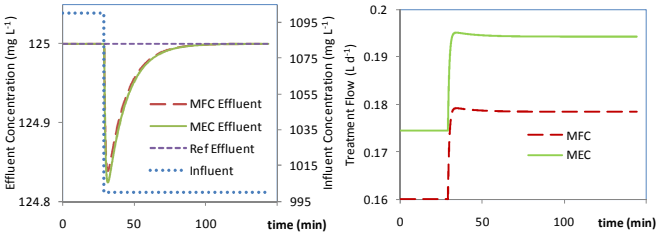

Figure 4. Treatment flow for 50 mL MEC and MFC with a PI controller. Influent was changed from 1100 mg-*A* L^{-1} to 1000 mg-*A* L^{-1} at 30 min. MFC's R_{ext} was set to 25 Ω, and MEC's applied voltage was set to 0.8 V.

As one can see, both systems showed very similar responses. New flow rates were reached in about 20 min, while the effluent concentration returned to its set-point in approximately 50 min. The MEC demonstrated slightly higher treatment capacity as compared to the MFC. This can be explained by the difference in kinetic constants (maximal reaction rates) estimated for the two modes of MxC operation.

5. CONCLUSIONS

This study presents a unified MxC model capable of simulating electricity production (MFC) as well as hydrogen production (MEC). Cathodic reactions in MFCs and MECs are represented by two distinctive electrochemical balances, while the same set of equations was used to describe anodic compartment balances. The previously developed MFC model was validated using a new data set thus confirming the

predictive power of the model. Furthermore, the MxC parameters were estimated using MEC tests and the model was successfully validated on the independent data set. An application of the resulting MxC model for process control purposes was demonstrated.

6. REFERENCES

Aelterman, P., M. Versichele, M. Marzorati, N. Boon and W. Verstraete. 2008. *Loading rate and external resistance control the electricity generation of microbial fuel cells with different three-dimensional anodes*. Bioresource Technology 99(18):8895-8902.

Batstone, D. J. , J. Keller, I Angelidaki, S. V. Kalyuzhnyi, S.G. Pavlostathis, A. Rozzi, W.T.M. Sanders, H. Siegrist and V. Vavilin. 2002. *Anaerobic digestion model no 1 (ADM1)*: IWA Publishing, London, UK.

Bond, D. R., D. E. Holmes, L. M. Tender and D. R. Lovley. 2002. *Electrode-reducing microorganisms that harvest energy from marine sediments*. Science 295(5554):483-485.

Logan, B. E., D. Call, S. Cheng, H. V. M. Hamelers, T. H. J. A. Sleutels, A. W. Jeremiasse and R. A. Rozendal. 2008. *Microbial Electrolysis Cells for High Yield Hydrogen Gas Production from Organic Matter*. Environmental Science & Technology 42(23):8630-8640.

Logan, B.E., B. Hamelers, R.A. Rozendal, U. Schroder, J. Keller, S. Freguia, P. Aelterman, W. Verstraete and K. Rabaey. 2006. *Microbial Fuel Cells: Methodology and Technology*. Environmental Science and Technology 40(17):5181-5192.

Manuel M.-F., Neburchilov V., Wang H., Guiot S. R. and Tartakovsky B. 2010. *Hydrogen production in a microbial electrolysis cell with nickel-based gas diffusion cathodes*. Journal of Power Sources 195(17):5514-5519.

Marcus, A. K., C. I. Torres and B. E. Rittmann. 2007. *Conduction-based modeling of the biofilm anode of a microbial fuel cell*. Biotechnology and Bioengineering 98(6):1171-1182.

National Energy Technology Laboratory, U.S. Department of Energy 2005. *Fuel Cell Handbook* 7th Edition: University Press of the Pacific.

Noren, D. A. and M. A. Hoffman. 2005. *Clarifying the Butler-Volmer equation and related approximations for calculating activation losses in solid oxide fuel cell models*. Journal of Power Sources 152(1-2):175-181.

Pinto, R. P., M. Perrier, B. Tartakovsky and B. Srinivasan. 2010a. *Performance analyses of microbial fuel cells operated in series.* In DYCOPS - Proceedings of 9th International Symposium on Dynamics and Control of Process Systems. Leuven, Belgium.

Pinto, R. P., B. Srinivasan, M. F. Manuel and B. Tartakovsky. 2010b. *A two-population bio-electrochemical model of a microbial fuel cell*. Bioresource Technology 101(14):5256-5265.

Pinto, R. P., B. Tartakovsky, M. Perrier and B. Srinivasan. 2010c. *Optimizing Treatment Performance of Microbial Fuel Cells by Reactor Staging*. Industrial & Engineering Chemistry Research 49(19):9222-9229.

Rauch, W., H. Vanhooren and P. A. Vanrolleghem. 1999. *A simplified mixed-culture biofilm model*. Water Research 33(9):2148-2162.

Reguera, G., K.D. McCarthy, T. Mehta, J.S. Nicoll, M.T. Tuominen and D.R. Lovley. 2005. *Extracellular electron transfer via microbial nanowires.* Nature Biotechnology 435:1098-1101.

Rozendal, R. A., H. V. M. Hamelers, G. J. W. Euverink, S. J. Metz and C. J. N. Buisman. 2006. *Principle and perspectives of hydrogen production through biocatalyzed electrolysis*. International Journal of Hydrogen Energy 31(12):1632-1640.

Wanner, O. and W. Gujer. 1986. *Multispecies Biofilm Model*. Biotechnology and Bioengineering 28(3):314-328.

Woodward, L., M. Perrier, B. Srinivasan, R. P. Pinto and B. Tartakovsky. 2010. *Comparison of real-time methods for maximizing power output in microbial fuel cells*. AIChE Journal 56(10):2742-2750.

Zeng, Y., Y. F. Choo, B.-H. Kim and P. Wu. 2010. *Modelling and simulation of two-chamber microbial fuel cell*. Journal of Power Sources 195(1):79-89.

7. APPENDIX

Table 2. Model parameters. Non-identified parameters were selected based on Pinto et al. (2010b) or Batstone et al. (2002).

	Param	Value	Description & Dimension
MxC	Y_{CH4}	0.28	methane yield - mL-CH_4 mg-A^{-1}
	$q_{max,m}$*	14.12	max. reaction rate- mg-*A* mg-$x^{-1}d^{-1}$
	$\mu_{max,a}$*	1.97	max. growth rate - d^{-1}
	$\mu_{max,m}$*	0.3	max. growth rate - d^{-1}
	$\mu_{max,h}$	0.5	max. growth rate - d^{-1}
	$K_{A,a}$	20	half-rate constant - mg-*A* L^{-1}
	$K_{A,m}$	80	half-rate constant - mg-*A* L^{-1}
	m	2	electrons transferred per mol of mediator - $mole^{-}$ mol_M^{-1}
	γ	663400	mediator *MM* - mg-*M* mol_M^{-1}
	M_{Total}	0.05	mediator fraction - mg-*M* mg-x^{-1}
	K_M	0.01	half-rate constant - mg-*M* L^{-1}
	$K_{d,a}$	0.04	decay rate - d^{-1}
	$K_{d,m}$	0.006	decay rate - d^{-1}
	$K_{d,h}$	0.01	decay rate - d^{-1}
	K_h	0.0001	half-rate constant - mg-*A* L^{-1}
	H_2^*	1	H_2 saturation in water - mg L^{-1}
	$Y_{H2/CH4}$	0.25	yield - mL-CH_4 mL-H_2^{-1}
	Y_{H2}	0.9	cathode efficiency
	$X_{max,1}$	512.5	max. biofilm density - mg-*x* L^{-1}
	R_{MIN}*	20	minimum internal resistance - Ω
	R_{MAX}	2000	maximum internal resistance - Ω
	K_R*	0.024	parameter Eqs. (25-26) - L mg-x^{-1}
MFC	$q_{max,a}$*	8.48	max reaction rate - mg-*A* mg- $x^{-1}d^{-1}$
	Y_M*	22.75	yield in Eq. (14) - mg-*M* mg-A^{-1}
	E_{MIN}	0.01	minimum E_{OCV} - V
	E_{MAX}	0.663	maximum E_{OCV} - V
MEC	$q_{max,a}$*	13.14	max reaction rate - mg-*A* mg-$x^{-1}d^{-1}$
	Y_M*	34.85	yield in Eq. (14) - mg-*M* mg-A^{-1}
	$(Y_h \cdot X_{max2})$*	1680	yield and max. biofilm density - mg-*x* L^{-1}
	E_{CEF}*	-0.35	counter-electromotive force - V
	β	0.5	Tafel coefficient
	I_0	0.005	exchange current density - A m^{-2}

* Parameters estimated in Pinto et al. (2010b) or in this paper